200812005A
200812005B

厚生労働科学研究費補助金

医療機器開発推進研究事業

蛋白質セラピー法とバイオナノカプセルによる持続性脳腫瘍治療薬の開発に関する研究

平成１８年度～２０年度
総合研究報告書

総括研究報告書

分担研究報告書

研究代表者　松井　秀樹

平成２１（２００９）年　３月

目　　次

厚生労働科学研究費補助金（医療機器開発推進研究事業）
Ⅱ．総括研究報告書

蛋白質セラピー法とバイオナノカプセルによる持続性脳腫瘍治療薬の開発

主任研究者　松井　秀樹　岡山大学大学院医歯薬学総合研究科・教授

抗癌剤ならびにボロンを封入した抗EGFR抗体付加型バイオナノカプセル(BNC)の開発に成功した。抗癌剤を封入したBNCに抗腫瘍効果があることを明らかにした。D-isomer型p53のC末端ペプチドにポリアルギニンとHA2を付加したペプチドを開発し、同ペプチドが脳腫瘍細胞のアポトーシスを誘導することを明らかにした。細胞膜透過性ボロン化合物の開発に成功した。

分担研究者
富澤一仁（熊本大院医学薬学・教授）
二木史郎（京都大院薬学・教授）
妹尾昌治（岡山大院自然科学・教授）
伊達　勲（岡山大院医歯薬学・教授）
上田政和（ピークル（株）・取締役）
宮武伸一（大阪医大医学部・准教授）

A．研究目的

「蛋白質セラピー法」と「徐放性バイオナノカプセル（BNC）」を組みあわせた悪性脳腫瘍治療法開発を行う。

B．研究方法

抗EGFR抗体を付加したBNCにドキソルビシンならびにボロン化合物のBSHを封入し、その抗腫瘍効果について検討した。p53 末端ペプチドにポリアルギニンならびにHA2を付加し、その脳腫瘍細胞の増殖抑制効果について検討した。

（倫理面への配慮）
動物実験は岡山大学動物実験委員会の許可を受けた後、指針に基づき実施した。

C．研究結果

抗EGFR抗体付加型BNCにドキソルビシンならびにBSHを封入することに成功した。ドキソルビシンを封入したBNCは脳腫瘍の抑制効果があった。p53末端ペプチドにポリアルギニンならびにHA2を付加加したペプチドを開発し、抗腫瘍効果を確認した。細胞膜透過性ボロン化合物を開発した。同化合物を株化脳腫瘍細胞の培地に添加し、その細胞内への導入効率ならびに細胞内局在について検討したところ腫瘍細胞内に効率よく導入されることが明らかになった。

D．考察

本研究により、3種類の新規化合物を作製することができた。抗EGFR抗体のBNCへの付加がBNCの脳腫瘍標的化に非常に有効であることが明らかになった。バリアントⅢ型EGFRは、正常細胞での発現はほとんど無いため、副作用の少ない脳腫瘍ター ゲティング技術として期待できる。

また、脳腫瘍に選択的に導入できるボロン化合物は、中性捕捉療法の中性子の効果を増幅させ、副作用を低下させることが期待できる。

E．結論

本研究で開発することに成功した3つの化合物が、ナノ医療の医薬品になり得ることを示すことができた。今後毒性試験などの前臨床試験を実施予定である。

F．健康危険情報

健康に害を及ぼすような事案は発生しなかった。

G．研究発表

1．論文発表

1. Tsutsui et al. Development of bionanocapsules targeting brain tumors. ***J Control Release*** 122, 159 (2007)
2. Feng et al. Delivery of sodium borocaptate to glioma cells using immunoliposome conjugated with anti-EGFR antibodies by ZZ-His. ***Biomaterials*** 30, 1746-1755 (2009)

H．知的財産権の出願・登録状況

現在のところ無し。

厚生労働科学研究費補助金（医療機器開発推進研究事業）
Ⅲ．分担研究報告書

1．蛋白質セラピー法とバイオナノカプセルによる持続性脳腫瘍治療薬の開発

分担研究者　富澤　一仁　熊本大学大学院医学薬学研究部・教授

抗EGFR抗体付加型バイオナノカプセル（BNC）に抗癌剤のドキソルビシンならびにボロン化合物であるBSHを封入することに成功した。さらにこれら抗癌剤ならびにBSH封入BNCが、脳腫瘍細胞であるGli36細胞に標的化することをin vitroで確認した。一方、正常細胞には、導入されなかった。

分担研究者：

省略

A．研究目的

脳腫瘍を標的化するバイオナノカプセルの開発、ならびに内因性ペプチド・蛋白分解酵素により分解されにくい細胞膜透過性抗腫瘍ペプチドの開発。

B．研究方法

リポソーム内にまずドキソルビシンあるいはBSHを封入し、その後同リポソームとBNCをカラムクロマトグラフにより混合した。抗癌剤、BSHの封入の確認は、分光高度計にて行った。さらに抗癌剤封入BNCが脳腫瘍細胞に標的化するか、脳腫瘍細胞のGli36細胞とラット正常グリア細胞への導入効率について生細胞イメージング法にて検討した

（倫理面への配慮）

該当事項無し。

C．研究結果

抗EGFR抗体を付加したBNCに抗癌剤のドキソルビシンをBNC1μgあたり0.48μg封入することに成功した。また抗癌剤封入BNCは脳腫瘍細胞には効率的に標的化するが、正常グリア細胞あるいは神経細胞には、ほとんど導入されなかった。

D．考察

抗EGFR抗体付加型BNCに抗癌剤ならびにボロン化合物を封入することに成功した。本研究成果は、副作用の少ない脳腫瘍化学療法や中性子捕捉療法の開発に繋がる成果である。今後、ボロン化合物を封入したバイオナノカプセルを脳腫瘍モデルマウスに投与後、加速器により中性子線を照射し、抗腫瘍効果について検討することが重要である。

E．結論

抗EGFR抗体付加型バイオナノカプセル（BNC）に抗癌剤のドキソルビシンならびにボロン化合物のBSHを封入することに成功した。またこれらナノメディシン薬剤が脳腫瘍細胞に標的化することを明らかにした。

F．健康危険情報

総括研究報告書参照

G．研究発表

1．論文発表

1. Wu Y. et al. Truncations of amphiphysin I by calpain inhibit vesicle endocytosis during neural hyperexcitation. ***EMBO J.*** 26, 2981-2990, 2007.

2. Kitani K. et al. A Cdk5 inhibitor enhances induction of insulin secretion by exendin-4 both in vitro and in vivo. ***J. Physiol. Sci.***, 57, 235-239, 2007.

3. Yamada H. et al. Amphiphysin I is important for actin polymerization duirng phagocytosis. ***Mol. Cell Biol.***, 18, 4669-4680, 2007

H．知的財産権の出願・登録状況

現在のところ無し。

厚生労働科学研究費補助金（医療機器開発推進研究事業）
Ⅲ．分担研究報告書

蛋白質セラピー法とバイオナノカプセルによる持続性脳腫瘍治療薬の開発

分担研究者　二木　史郎　京都大学大学院薬学研究科・教授

ヒトp53のC端ペプチドのD-isomerに、更に新たに開発した膜透過促進配列ペプチドとR11やFHVなどの膜透過ペプチドの融合ペプチドを付加することにより、長期間効果を持続する細胞移行性抗腫瘍ペプチドの創製に成功した。

分担研究者：

省略

A．研究目的

タンパク質セラピー法によるガン抑制蛋白質のガン細胞への特異的・効率的導入と抗ガン効果の飛躍的な向上と分子サイズの低減を目指し、新たに開発した膜透過促進配列ペプチドとR11をはじめとしたポリアルギニンやFHVなどの膜透過ペプチドの併用による光学異性体型p53 C末端ペプチドの効果の向上を目指す。

B．研究方法

ヒトp53アミノ酸配列の361ー382番目に相当するペプチドに、膜透過促進配列ペプチドと膜透過ペプチドの融合ペプチドを付加したD-isomerペプチドを合成し、活性増強を試みた。

（倫理面への配慮）
該当事項無し。

C．研究結果

ペプチドを脳腫瘍モデルとしてのA172、T98G、あるいはU251MGグリオーマ細胞に導入し、その導入効率、また細胞増殖抑制効果についてWST-1アッセイにて検討した。0.1 μMならびに1 μMの濃度で膜透過性D-isomer p53 C末端ペプチドをほぼすべてのグリア細胞に導入することができた。また、膜透過促進配列ペプチドとR11あるいはFHVペプチドの融合ペプチドの付加によりD-isomer p53 C末端ペプチドは1日目に投与すると、その抗腫瘍効果が4日間持続することが確認できた。10 μMのペプチドを投与した場合には、4日後においても、グリオーマ細胞の増殖は認められず、膜透過促進配列ペプチドとのハイブリは脳腫瘍細胞増殖抑制に有効であることが示唆された。

D．考察

膜透過促進配列ペプチドとR11やFHVなどの膜透過ペプチドの融合ペプチドにより、細胞取り込み効果とエンドソーム脱出効果が向上し、光学異性体型p53 C末端ペプチドの腫瘍細胞増殖抑制効果が著しく高まることが分かった。

E．結論

膜透過促進配列ペプチドとR11やFHVなどの膜透過ペプチドの融合ペプチドを用いることにより、効率よく腫瘍内に導入でき、また腫瘍細胞内で分解されず長期間抗腫瘍効果を持続できる高活性の膜透過性D-isomer p53 C末端ペプチドの開発に成功した。

F．健康危険情報
総括研究報告書参照

G．研究発表
1．論文発表

1. Futaki S & Asami K. Ligand-induced extramembrane conformation switch controlling alamethicin assembly and the channel current. ***Chem Biodivers***. 4, 1313 (2007).

H．知的財産権の出願・登録状況
現在のところ無し。

厚生労働科学研究費補助金（医療機器開発推進研究事業）
Ⅲ．分担研究報告書

蛋白質セラピー法とバイオナノカプセルによる持続性脳腫瘍治療薬の開発

分担研究者　妹尾　昌治　岡山大学大学院自然科学研究科・教授

ドキソルビシンを封入した抗EGFR抗体付加BNCの脳腫瘍細胞に対する抗腫瘍効果について実証した。同BNCは、脳腫瘍細胞株化細胞であるGli36細胞の増殖を濃度依存的に抑制することを明らかにした。

分担研究者：

省略

A．研究目的

脳腫瘍に特異的に導入されるBNCの開発を行う。

B．研究方法

BNCのプレS1領域をprotein Aで置換し、BNCの肝細胞標的化能力を喪失させ、抗体が結合できるBNCの作製を行った。そしてバリアントⅢ型EGF受容体を特異的に認識するモノクローナル抗体をBNCに結合させた。

脳腫瘍患者から株化したGli36細胞に0.1ー10μg/ml濃度のドキソルビシン封入BNC（EGFR抗体付加、同抗体付加無し）を培地に添加し、細胞増殖抑制効果についてWSTアッセイにて検討した。またEGFR抗体付加ならびにEGFR抗体付加無しで細胞増殖抑制効果に差があるか比較検討した。

（倫理面への配慮）

該当事項無し。

C．研究結果

BNCのプレS1領域をprotein Aで置換することにより様々な抗体をBNCに付加できることを確認した。

ドキソルビシン封入BNCは、ドキソルビシン未封入BNCと比較して、脳腫瘍細胞の増殖を有意に抑制した。また各濃度の抗腫瘍効果について検討した結果、濃度依存的に脳腫瘍の増殖を抑制した。

さらに、抗EGFR抗体を付加したBNCと付加していないBNCで比較検討したところ、脳腫瘍細胞増殖抑制効果に差は認められなかった。また、ドキソルビシン封入BNCを投与された脳腫瘍細胞では、増殖抑制効果が見られた。

D．考察

ドキソルビシンを封入したBNCには、強い抗腫瘍効果があることが示唆された。抗EGFR抗体付加BNCは、腫瘍ターゲティング作用があり、ドキソルビシンを封入した抗EGFR抗体付加BNCには、脳腫瘍細胞を選択的に死滅させる効果が期待できることが考察された。

E．結論

ドキソルビシンを封入した抗EGFR抗体付加BNCは、脳腫瘍細胞に対する抗腫瘍効果を有していることを明らかにした。

F．健康危険情報

総括研究報告書参照

G．研究発表

1．論文発表

1. Watanabe K. et al. Involvement of MAPK signaling molecules and Runx2 in the NELL1-induced osteoblastic differentiation. J. Biol. Chem. 282: 31643 (2007).

2. Nagaoka T. et al. Characterization of bio-nanocapsule as a transfer vector targeting human hepatocyte carcinoma by disulfide linkage modification. ***J. Control. Release*** 118: 348 (2007)

H．知的財産権の出願・登録状況

現在のところ無し。

厚生労働科学研究費補助金（医療機器開発推進研究事業）
Ⅲ．分担研究報告書

蛋白質セラピー法とバイオナノカプセルによる持続性脳腫瘍治療薬の開発

分担研究者　伊達　勲　岡山大学大学院医歯薬学総合研究科・教授

ボロン化合物であるBSHにポリアルギニンもしくはSV40の核移行シグナルを付加したBSH化合物が、腫瘍細胞に効率的に導入されることを明らかにした。また浸潤性に増殖する脳腫瘍モデルマウスの作製を行った。

分担研究者：

省略

A．研究目的

内因性ペプチド・蛋白分解酵素により分解されにくいD-isomer型細胞膜透過性p53ペプチドの抗腫瘍効果の検討。本研究で開発したBNCならびにD-isomerペプチドのin vivo抗腫瘍効果を検討するための脳腫瘍モデルマウスの作製。

B．研究方法

大阪医科大学で作製したBSHにポリアルギニンもしくはSV40の核移行シグナルを付加したBSH化合物が、脳腫瘍細胞内に導入されるかGli36細胞を用いて検討した。

0.1 μMならびに1 μM濃度のBSH化合物を培地に添加し、洗浄後共焦点レーザー顕微鏡によるイメージング法にて細胞内の局在について検討した。

（倫理面への配慮）

動物実験は岡山大学動物実験委員会の許可を受けた後、岡山大学動物実験指針に基づき実施した。

C．研究結果

0.1 μMならびに1 μMのポリアルギニンもしくは核移行シグナルを付加したBSH化合物は、効率良く脳腫瘍細胞内に導入されることが確認された。一方、ペプチドを付加していないBSHでは、全く細胞内に導入されなかった。

ポリアルギニンを付加したBSHが、核移行シグナルを付加したペプチドより効率的に細胞内に導入された。

変異型p53を強制発現させたマウスの線条体にマウスグリオーマ細胞を植立することにより浸潤性に増殖する脳腫瘍モデルマウスを作製することに成功した。

D．考察

ポリアルギニンを付加したBSH化合物が腫瘍細胞内に効率よく導入されたことから、この新規膜透過性BSHが脳腫瘍に対する中性子捕捉療法に応用できることが示唆された。

E．結論

ボロン化合物であるBSHにポリアルギニンもしくはSV40の核移行シグナルを付加したBSH化合物が、腫瘍細胞に効率的に導入されることを明らかになった。

F．健康危険情報

総括研究報告書参照

G．研究発表

1．論文発表

1. Iseda K et al. Antivasospastic and antiinflammatory effects of caspase inhibitor in experimental subarachnoid hemorrhage. ***J Neurosurg***. 107:128 (2007).

H．知的財産権の出願・登録状況

現在のところ無し。

厚生労働科学研究費補助金（医療機器開発推進研究事業）
Ⅲ．分担研究報告書

蛋白質セラピー法とバイオナノカプセルによる持続性脳腫瘍治療薬の開発

分担研究者　上田　政和　株式会社ビークル・取締役

光学異性体型ヒトp53のC端ペプチドに膜透過性ペプチドを付加した膜透過性抗腫瘍性ペプチドにさらにインフルエンザウイルスが発現するヘマングルチニンサブユニットペプチド（HA2）を付加したペプチドが抗腫瘍効果を有することを明らかにした。

分担研究者：

省略

A．研究目的

抗腫瘍効果を有する膜透過性ペプチドの作製。

B．研究方法

京都大学で作製した膜透過性光学異性体型ヒトp53のC端ペプチドにHA2を付加したペプチドを株化脳腫瘍細胞の培地に添加し、その細胞内局在について細細胞イメージング法にて検討した。また同ペプチドの細胞増殖抑制効果ならびにアポトーシス誘導効果についてWSTアッセイ、TUNEL染色にて検討した。

（倫理面への配慮）

該当事項無し。

C．研究結果

HA2を付加していない膜透過性光学異性体型ヒトp53のC端ペプチドは、脳腫瘍細胞内においてマクロピノソーム内で停留していた。一方、HA2を付加したペプチドは、脳腫瘍細胞の細胞質ならびに核内に局在していることが明らかになった。

また、HA2を付加していない膜透過性光学異性体型ヒトp53のC端ペプチドの腫瘍抑制効果は弱かったが、HA2を付加した膜透過性光学異性体型ヒトp53のC端ペプチドは、強い腫瘍増殖抑制効果を示した。また腫瘍細胞のアポトーシスも促進することが明らかになった。

D．考察

光学異性体型ヒトp53のC端ペプチドに膜透過性ペプチドを付加した膜透過性抗腫瘍性ペプチドにさらにHA2を付加したペプチドが抗腫瘍効果を示したことから、本ペプチドが長期持続的に抗腫瘍効果を発揮する脳腫瘍治療薬になる可能性が示唆された。

E．結論

光学異性体型ヒトp53のC端ペプチドに膜透過性ペプチドを付加した膜透過性抗腫瘍性ペプチドにさらにHA2を付加したペプチドが抗腫瘍効果を有することが明らかになった。

F．健康危険情報

総括研究報告書参照

G．研究発表

1．　論文発表

1. Akatsu T et al. Pseudoaneurysm of the cystic artery secondary to cholecystitis as a cause of hemobilia: report of a case ***Surg. Today***. 37: 412-417 (2007)

2. Akatsu T et al. Duodenal gastrointestinal stromal tumor adjacent to the minor papilla with concomitant pancreatic divisum. ***Dig. Sis. Sci.*** 52: 3191-3198 (2007)

H．知的財産権の出願・登録状況

現在のところ無し。

厚生労働科学研究費補助金（医療機器開発推進研究事業）
Ⅲ．分担研究報告書

蛋白質セラピー法とバイオナノカプセルによる持続性脳腫瘍治療薬の開発

分担研究者　宮武　伸一　大阪医科大学・准教授

新規ホウ素製剤の創出。ボロン化合物の一種であるBSHにポリアルギニンもしくはSV-40が有する核移行シグナルを付加したBSH化合物の開発を行った。

分担研究者：

省略

A．研究目的

脳腫瘍に対する中性子捕捉療法に応用できる。腫瘍細胞膜透過性BSH化合物の開発

B．研究方法

以下の2種類のペプチド合成を行った。
① RRRRRRRRRRR（ポリアルギニン）
② PKKKRKV（核移行シグナルペプチド）
のN末端にCysを付加し、さらにNpys基、マレイミド化したペプチドの合成。

これらペプチドとBSHを液相、25℃で6時間、酸化反応することによりBSHに各ペプチドを付加した。その後カラムクロマトグラフィーにより精製し、未反応のBSH、ペプチドを除去した。BSHにペプチドが付加できているか液クロ、質量分析装置にて解析した。

（倫理面への配慮）
該当事項無し。

C．研究結果

BSHにポリアルギニンペプチドならびに核移行シグナルペプチドをジスルフィド結合により付加することに成功した。開発BSH化合物が常温にて安定であることを明らかにした。また従来のBSHと比較し易水溶性であることを明らかにした。

D．考察

悪性グリオーマの浸潤に対しては有効な治療が現在のところ存在しない。今回の我々の研究結果は、そのような悪性グリオーマの治療に対し、ホウ素中性子捕捉療法を行う上で一つの解決策を示す重要な研究であると考えられた。

E．結論

ボロン化合物の一種であるBSHにポリアルギニンもしくはSV-40が有する核移行シグナルを付加したBSH化合物の作製に成功した。細胞膜通過ペプチドを有するBSHは、細胞内へ導入され、新規ホウ素製剤となる可能性を示した。

F．健康危険情報

総括研究報告書参照

G．研究発表

1．論文発表

1. Miyatake S et al. Boron neutron capture therapy for malignant tumors related to meningiomas. ***Neurosurgery*** 61: 82-90 (2007)

2. Ariyoshi Y et al. Boron neutron capture therapy using epithermal neutrons for recurrent cancer in the oral cavity and cervical lymph node metastasis. ***Oncol. Rep.*** 18: 861-866 (2007)

H．知的財産権の出願・登録状況

現在のところ無し。

Ⅳ. 研究成果の刊行に関する一覧表

書籍

該当無し

雑誌

発表者氏名	論文タイトル名	発表誌名	巻号	ページ	出版年
Kuriyama M. et al.	A cell-permeable NFAT inhibitor peptide prevents pressure-overload cardiac hypertrophy.	Chem. Biol. Drug Des.	67	238 -243	2006
Inoue M. et al.	p53 protein transduction therapy: Successful targeting and inhibition of the growth of the bladder cancer cells	Eur. Urol.	49	161 -168	2006
Yagi H. et al.	Anti-tumor effect in an in vivo model by human-derived pancreatic RNase with basic fibroblast growth factor insertional fusion protein through antiangiogenic properties.	Cancer Sci.	97	1315 -1320	2006
Shishido T. et al.	Secretory production system of bionanocapsules using a stably transfected insect cell line.	Appl. Microbiol. Biotechnol.	73	505 -511	2006
Murata H. et al.	Denatured and Reversibly Cationized p53 Readily Enters Cells and Simultaneously Folds to the Functional Protein in the Cells.	Biochemistry	45	6124 -6132	2006
Sanderson M.P. et al.	Hydrogen peroxide and endothelin-1 are novel activators of betacellulin ectodomain shedding.	J. Cell Biochem.	99	609 -623	2006
Hoshimoto S. et al.	Mechanisms of the growth-inhibitory effect of the RNase-EGF fused protein against EGFR-overexpressing cells.	Anticancer Res.	26	857 -863	2006
Yu D. et al.	Engineered bio-nanocapsules, the selective vector for drug delivery system.	IUBMB Life.	58	1-6	2006
Kameyama S. et al.	Distribution of Immunoglobulin Fab Fragment Conjugated with HIV-1 REV Peptide Following Intravenous Administration in Rats.	Mol. Pharm.	3	174 -180	2006
Akita H. et al.	Evaluation of the Nuclear Delivery and Intra-nuclear Transcription of Plasmid DNA Condensed with m (mu) and NLS-m by Cytoplasmic and Nuclear Microinjection: A Comparative Study with Poly-L-lysine	J. Gene Med.	8	198 -206	2006
Ikramy A. et al.	High Density of Octaarginine Stimulates Macropinocytosis Leading to Efficient Intracellular Trafficking for Gene Expression.	J. Biol. Chem.	281	3544 -3551	2006
Al-Taei S. et al.	Intracellular Traffic and Fate of Protein Transduction Domains HIV-1 TAT Peptide and Octaarginine. Implications for their Utilization as Drug Delivery	Bioconjug. Chem.	17	90 -100	2006
Nakamura Y. et al.	Significant and Prolonged Antisense Effect of a Multifunctional Envelope-type Nano Device Encapsulating Antisense Oligodeoxynucleotide.	J. Pharm. Pharmacol.	58	431 -437	2006

Nakamura T. et al	Delivery of Condensed DNA by Liposomal Non-viral Gene Delivery System into Nucleus of Dendritic Cells	Biol. Pharm. Bull.	29	1290 -1293	2006
Iwasa A. et al.	Cellular Uptake and Subsequent Intracellular Trafficking of R8-liposomes Introduced at Low Temperature.	Biochim. Biophys. Acta–Biomembranes	1758	713 -720	2006
Kobayashi K. et al.	Control of dopamine-secretion by Tet-Off system in an in vivo model of parkinsonian rat.	Brain Res.	1102	1-11	2006
Tamiya T. et al.	Successful chemotherapy for congenital malignant gliomas: a report of two cases.	Pediatr. Neurosurg.	42	240 -244	2006
Yasuhara T. et al.	Ex vivo gene therapy: transplantation of neurotrophic factor-secreting cells for cerebral ischemia.	Front Biosci.	11	760 -775	2006
Satoh T. et al.	Differential diagnosis of the infundibular dilation and aneurysm of internal carotid artery: assessment with fusion imaging of 3D MR cisternography/angiography.	AJNR Am. J. Neuroradiol.	27	306 -312	2006
Tokunaga K. et al.	Transient memory disturbance after removal of an intraventricular trigonal meningioma by a parieto-occipital interhemispheric precuneus approach.	Surg. Neurol.	65	167 -169	2006
Muraoka K. et al.	The high integration and differentiation potential of autologous neural stem cell transplantation compared with allogeneic transplantation in adult rat hippocampus.	Exp. Neurol.	199	311 -327	2006
Ogawa N. et al.	Novel protein transduction method by using 11R. An effective new drug delivery system fro the treatment of cerebrovascular diseases.	Stroke	38	1354 -1361	2007
Nakase I. et al.	Interaction of arginine-rich peptides with membrane-associated proteoglycans is crucial for induction of actin organization and macropinocytosis.	Biochemistry	46	492-501	2007
Miyatake S. et al.	Fluorescence of non-neoplastic, magnetic resonance imaging-enhancing tissue by 5-aminolevulinic acid: case report.	Neurosurgery	61	E1101-1103	2007
Miki Y. et al.	Vascular endothelial growth factor gene-transferred bone marrow stromal cells engineered with a herpes simplex virus type 1 vector can improve neurological deficits and reduce infarction volume in rat brain ischemia.	Neurosurgery	61	586-594	2007
Ariyoshi Y. et al.	Boron neuron capture therapy using epithermal neutrons for recurrent cancer in the oral cavity and cervical lymph node metastasis.	Oncol. Rep.	18	861-866	2007
Iwasaki Y. et al.	Gene therapy of liver tumors with human liver-specific nanoparticles.	Cancer Gene Ther.	14	74-81	2007
Miyatake S. et al.	Boron neutron capture therapy for malignant tumors related to meningiomas.	Neurosurgery.	61	82-90	2007
Tanaka H. et al.	Inhibition of matrix metalloproteinase-9 activity by trandolapril after middle cerebral artery occlusion in rats.	Hypertens. Res.	30	469-475	2007

Kajimoto Y. et al.	Use of 5-aminolevulinic acid in fluorescence-guided resection of meningioma with high risk of recurrence. Case report.	J. Neurosurg.	106	1070-1074	2007
Tamura Y. et al.	Endoscopic identification and biopsy sampling of an intraventricular malignant glioma using a 5-aminolevulinic acid-induced protoporphyrin IX fluorescence imaging system. Technical note.	J. Neurosurg.	106	507-510	2007
Inoue H. et al.	Massive apoptotic cell death of human glioma cells via a mitochondrial pathway following 5-aminolevulinic acid-mediated photodynamic therapy.	J. Neurooncol.	83	223-231	2007
Yokoyama K. et al.	Analysis of boron distribution in vivo for boron neutron capture therapy using two different boron compounds by secondary ion mass spectrometry.	Radiat. Res.	167	102-109	2007
Han X.-J. et al.	CaM kinase 1a-induced phsophorylation of DRP1 regulates mitochondrial morphology.	J. Cell Biol.	182	573-585	2008
Han X.-J. et al.	Involvement of calcineurin in glutamate-induced mitochondrial dynamics in neurons.	Neurosci. Res.	60	114-119	2008
Ohmori I. et al.	A CACNB4 mutation shows that altered Ca(v)2.1 function may be a genetic modifier of severe myoclonic epilepsy in infancy.	Neurobiol. Dis.	32	349-354	2008
Doi A. et al.	Tumor-specific targeting of sodium borocaptate (BSH) to malignant glioma by transferrin-PEG liposomes for boron neutron capture therapy.	J. Neurooncol.	87	287-294	2008
Miyashita M. et al.	Evaluation of Fluoride-labeled Boronophenylalanine-PET Imaging for the Study of Radiation Effects in Patients with Malignant Gliomas.	J. Neuro.-Oncol.	89	239-246	2008
Takahashi K. et al.	Embryonic neural stem cells transplanted in middle cerebral artery occlusion model of rats demonstrated potent therapeutic effects, compared to adult neural stem cells	Brain Research	1234	172-182	2008
Agari T. et al.	Intrapallidal metabotropic glutamate receptor activation in a rat model of Parkinson's disease: behavioral and histological analyses.	Brain Research	1203	189-96	2008
Hishikawa T. et al.	Effects of deferoxamine-activated hypoxia-inducible factor-1 on the brainstem after subarachnoid hemorrhage in rats.	Neurosurgery	62	232-40	2008
Muraoka K. et al.	Comparison of the therapeutic potential of adult and embryonic neural precursor cells in a rat model of Parkinson disease.	J. Neurosurgery	108	149-59	2008
Bin F. et al.	Delivery of sodium borocaptate to glioma cells using immunoliposome conjugated with anti-EGFR antibodies by ZZ-His.	Biomaterials	30	1746-1755	2009
Kimura Y	Boron Neutron Capture Therapy for Papillary Cystadenocarcinoma in the Upper Lip.	Int. J. Oral & Maxillo. Surgery	38	293-295	2009

THE JOURNAL OF GENE MEDICINE
J Gene Med 2006; **8**: 198–206.
Published online 14 November 2005 in Wiley InterScience (www.interscience.wiley.com). **DOI:** 10.1002/jgm.839

RESEARCH ARTICLE

Evaluation of the nuclear delivery and intra-nuclear transcription of plasmid DNA condensed with μ (mu) and NLS-μ by cytoplasmic and nuclear microinjection: a comparative study with poly-L-lysine

Hidetaka Akita[1,3]*
Mitsuhide Tanimoto[1]
Tomoya Masuda[1,3]
Kentaro Kogure[1,3]
Susumu Hama[1,3]
Keiko Ninomiya[2,4]
Shiroh Futaki[2,4]
Hideyoshi Harashima[1,3]

[1]*Graduate School of Pharmaceutical Sciences, Hokkaido University, Sapporo, Hokkaido, Japan*

[2]*Institute for Chemical Research, Kyoto University, Uji, Kyoto, Japan*

[3]*CREST, Japan Science and Technology Corporation (JST), Japan*

[4]*PRESTO, Japan Science and Technology Corporation (JST), Japan*

*Correspondence to:
Hidetaka Akita, Laboratory for Molecular Design of Pharmaceutics, Graduate School of Pharmaceutics, Hokkaido University, Sapporo, Hokkaido 060-0812, Japan.
E-mail: akita@pharm.hokudai.ac.jp

Received: 7 February 2005
Revised: 16 July 2005
Accepted: 12 August 2005

Abstract

Background The efficient nuclear delivery of plasmid DNA (pDNA) is essential for the development of a promising non-viral gene vector. In an attempt to achieve nuclear delivery, NLS-mu, a novel pDNA condenser, was prepared. This consists of mu, a highly potent polypeptide for condensing the pDNA, and a SV40 T antigen-derived nuclear localization signal (NLS_{SV40}).

Methods The utility of NLS-mu was assessed in terms of green fluorescent protein (GFP) expression after cytoplasmic and nuclear microinjection of GFP-encoding pDNA along with the transfection, and compared with mu and poly-L-lysine (PLL). Trans-gene expression after cytoplasmic microinjection was affected by the efficiencies of nuclear transfer and following intra-nuclear transcription. To evaluate the nuclear transfer process separately, we introduced a parameter, a nuclear transfer score (NT score), which was calculated as the trans-gene expression after cytoplasmic microinjection divided by that after nuclear microinjection.

Results As expected, the rank order of trans-gene expression after the transfection and cytoplasmic microinjection was NLS-mu > mu > PLL. However, the calculated NT scores were unexpectedly ranked as mu = NLS-mu > PLL, suggesting that mu, and not NLS_{SV40}, is responsible for the nuclear delivery of pDNA. In addition, confocal images of rhodamine-labeled pDNA indicated that pDNA condensed with mu and NLS-mu was delivered as a condensed form. In comparing the nuclear transcription, the rank order of trans-gene expression after nuclear microinjection was PLL = NLS-mu > mu, suggesting that intra-nuclear transcription is inhibited by efficient condensation by mu, and is avoided by the attachment of NLS_{SV40}.

Conclusions Collectively, NLS-mu, which consists of chimeric functions, is an excellent DNA condenser, and the process is based on mu-derived nuclear transfer and NLS_{SV40}-derived efficient intra-nuclear transcription. Copyright © 2005 John Wiley & Sons, Ltd.

Keywords nuclear delivery; plasmid DNA; microinjection; mu; nuclear localization signal

Introduction

The utility of a non-viral vector is hampered by low transfection efficiency in spite of the many potent advantages that include a lower immunogenicity and oncogenicity. For non-viral vectors, a critical rate-limiting step that interrupts efficient trans-gene expression is the process of the nuclear transfer of plasmid DNA (pDNA) [1,2]. This is supported by various observations showing that trans-gene expression is drastically enhanced at the M-phase when the nuclear membrane structure is perturbed [3–6]. In addition, a comparison of the dose-response curves for trans-gene expression after the nuclear and cytoplasmic microinjection of naked pDNA indicates that less than 1% of the cytoplasm-microinjected DNA actually reaches the nucleus [7]. Therefore, efficient systems for the nuclear delivery of pDNA would be highly desirable in ongoing attempts to develop an efficient gene delivery system.

Various attempts have been made to overcome the nuclear barrier with the expected function of the SV40 T antigen-derived nuclear localization signal (NLS_{SV40}). However, direct chemical modification of the NLS_{SV40} to the pDNA appears to have only a negligible effect on trans-gene expression [8,9]. This can be attributed to electrostatic interactions between the pDNA and the NLS_{SV40}, which interrupts the recognition of the NLS_{SV40} by importin α.

In the present study, we report on the synthesis of a novel polycation, NLS-mu, which has the expected heterogenic characteristics. In this peptide, NLS_{SV40} was modified on the μ (mu) peptide, which plays an important role in condensing the huge adenovirus genome (~36 kbp) into the adenovirus core structure, which has a diameter of 90 nm. The findings show that the particle size of pDNA prepared with mu was significantly smaller than that prepared with NLS_{SV40}, suggesting that mu may condense pDNA more efficiently than NLS_{SV40} presumably due to its high affinity to DNA [10]. We assumed, therefore, that the mu domain would preferentially condense pDNA by virtue of its strong interactions with pDNA, and it permits NLS_{SV40} to be partially displayed on the surface of the particle, thereby allowing its interaction with importin, although partial NLS_{SV40} also electrostatically interacts with pDNA.

We first compared the utility of NLS-mu in delivering the pDNA to the nucleus by means of transfection, and compared this process with mu and poly-L-lysine (PLL). The potential of NLS-mu for the nuclear delivery of pDNA was more directly comparable to mu and PLL by cytoplasmic and nuclear microinjection.

Materials and methods

General

HeLa cells were obtained from the RIKEN Cell Bank (Tsukuba, Japan). To prepare the reporter gene vector for the pDNA, an insert fragment encoding the enhanced green fluorescent protein (EGFP) was obtained by the EcoRI/Not I digestion of pEGFP-N1 (Clontech, Palo Alto, CA, USA), and ligated to the EcoRI/Not I digested site of pcDNA3.1 (Invitrogen, Carlsbad, CA, USA). Similarly, to prepare the luciferase-encoding vector, an insert fragment encoding the luciferase (GL3) was obtained by the Hind III/Xba I digestion of the pGL3 basic vector (Promega, Madison, WI, USA), and ligated to the HindIII/Xba I digested site of pcDNA3.1 (Invitrogen). Plasmids were purified with a Qiagen (Valencia, CA, USA) EndoFree™ Plasmid Mega kit. The mu peptide and NLS-mu peptide, as shown in Table 1, were obtained from Sigma Genosys Japan (Ishikari, Japan) in purified form. Poly-L-lysine (PLL, MW = 27 400) and cholesteryl hemisuccinate (CHEMS) were obtained from Sigma-Aldrich (St. Louis, MO, USA). Tetramethylrhodamine-labeled dextran (RhoDex: MW = 70 000) was purchased from Molecular Probes (Eugene, OR, USA). Dioleoylphosphatidylethanolamine (DOPE) was purchased from Avanti Polar Lipids (Alabaster, AL, USA). Other chemicals were commercially available and were reagent-grade products.

Preparation of the polycation/pDNA complex

For the condensation of pDNA, naked pDNA solution (100 μl, 0.1 μg/μl in H_2O) was added to 100 μl of polycation solution. The concentration of the NLS-mu, mu and PLL (C_p) at various charge ratios (+/−) was calculated using the following equation:

$$\text{Charge ratio}(+/-) = \{C_p \times (n_K + n_R)/MW_p\}/(C_D/MW_D)$$

where n_K and n_R denote the numbers of lysine and arginine residues in the polycation molecule. MW_P and MW_D denote the molecular weights of the polycation (NLS-mu: 3810.5, mu: 2440.89, PLL: 27 400) and one nucleotide (average: 308), respectively. C_D denotes the concentration of pDNA (0.1 μg/μl).

The hydrodynamic diameter was measured by quasi-elastic light scattering by means of an electrophoresis light-scattering spectrophotometer (ELS-8000; Otsuka Electronics, Japan).

Transfection experiment

The transfection study was demonstrated by a recently developed multifunctional envelope-type nano device (MEND). Preparation of the MEND and the luciferase assay have been described previously [11]. pDNA

Table 1. Amino acid sequences used in the present study

Peptide	Sequence
mu	NH_2-MRRAHHRRRRASHRRMRGG-COOH
NLS-mu	NH_2-PKKKRKVEDPYMRRAHHRRRRASHRRMRGG-COOH

(0.1 mg/ml) was first condensed with the NLS-mu, mu and PLL by mixing equal volumes of these solutions at a charge ratio of 2 by voltexing at room temperature. After the condensation, a lipid film was produced by evaporation of a chloroform solution of 137.5 nmol lipids (DOPE/CHEMS = 9:2 (molar ratio)) on the bottom of a glass tube. Then, 0.25 ml of the complex solution was applied, followed by incubation for 10 min to hydrate the lipid. The final solution of the lipid was 0.55 mM. The hydrated solution was sonicated in a bath-type sonicator (125 W; Branson Ultrasonics, Danbury, CT, USA) to complete the packaging.

Samples containing 0.4 μg DNA, suspended in 0.25 ml of serum- and antibiotics-free Dulbecco's modified Eagle's medium (DMEM), were added to 4×10^4 HeLa cells, followed by incubation for 3 h at 37 °C. Then, 1 ml of DMEM containing 10% fetal calf serum (FCS) was added to the cells, followed by further incubation for 45 h. The cells were then washed, and lysed with reporter lysis buffer (Promega). Luciferase activity was initiated by the addition of 50 μl of luciferase assay reagent (Promega) into 20 μl of the cell lysates, and measured by means of a luminometer (Luminescencer-PSN; ATTO, Japan). The amount of protein in the cell lysates was determined using a BCA protein assay kit (Pierce, Rockford, IL, USA).

Microinjection study

One day before the microinjection, cells were seeded on a glass-based dish (Iwaki, Osaka, Japan). For this procedure, a semiautomatic injection system (Eppendorf transjector 5246; Hamburg, Germany) attached to an Eppendorf micromanipulator 5171 was used. Cytoplasmic and nuclear microinjection was performed with the setting of Pi = 50–70 hPa, Pc = 30 hPa and an injection time of 0.2 s.

For the quantitative evaluation of transgene expression, the polycation/pDNA complex was diluted with 0.5% RhoDex/H_2O solution for the cytoplasmic or nuclear microinjection, respectively. At 24 h post-injection, GFP expression was monitored by fluorescence microscopy, and the ratio of cells expressing GFP to RhoDex-positive cells was calculated. In the case of nuclear microinjection, the rhodamine-positive cells were counted immediately after microinjection to avoid a situation where the RhoDex could diffuse into the cytosol during the 24 h incubation, leading to an underestimation of the number of nucleus-injected cells.

If pDNA was overdosed, trans-gene expression could become saturated, and therefore differences among NLS-mu, mu and PLL would be underestimated. To avoid this situation, we observed the relationship between the dose and trans-gene expression after cytoplasmic and nuclear microinjection of NLS-mu/pDNA particles in a preliminary experiment. As a result, the transfection efficiency after cytoplasmic and nuclear injection was linearly increased when the concentration of injected pDNA was in the range of 0.33–3.3 fmol/μl and 10–100 amol/μl, respectively (data not shown). Therefore, concentrations of injected samples were fixed at 3.3 fmol/μl and 33 amol/μl for cytoplasmic and nuclear injection, respectively.

The efficiency of a polycation/pDNA complex to pass through the microinjector was monitored in terms of the fluorescence signal of RhoDex in injected cells. If the efficiency of the polyplex to pass through the microinjector varies as a function of the polycation used, it should reflect the injected sample volume, resulting in a variation in the fluorescence of the injected RhoDex. After the injection of samples, fluorescence images were captured by fluorescence microscopy (Axioplan II, Carl Zeiss Co. Ltd.; Jena, Germany). Each 8-bit TIFF image was transferred to an Image-Pro Plus version 4.0 (Media Cybernetics Inc., Silver Spring, MD, USA) to quantify the brightness of the rhodamine signal in individual cells. As a result, the fluorescence signal of RhoDex was clearly observed in >80% of the injected cells for all polycations tested. Furthermore, the total brightness per cell was also comparable among the polyplexes ($4.0 \pm 1.2 \times 10^5$, $4.9 \pm 2.4 \times 10^5$ and $5.5 \pm 2.2 \times 10^5$ brightness/cell in mu, NLS-mu and PLL, respectively). Collectively, these findings confirm that the efficiency of polyplexes to pass through the injector was comparable.

For visualization of the pDNA after cytoplasmic injection, pDNA was labeled with rhodamine by the Label IT reagent (Panvera Corporation, Madison, WI, USA). One hour post-injection, the cells were incubated with 0.5 μM SYTO24 for 15 min to stain the nucleus. The cells were then washed three times with culture medium including 10% FCS. Fluorescence and bright field images were captured using a Zeiss Axiovert 200 inverted fluorescence microscope equipped with Achroplan 63 × /0.95 N objective (Carl Zeiss Co. Ltd.).

Evaluation of protection activity of polycations from enzymatic digestion of pDNA by DNase I

pDNA (0.4 μg) was condensed with various polycations at charge ratio of 2, and then treated with 0.05 U of DNase I (Roche Diagnostics) in 10 μl of reaction buffer (5 mM $MgCl_2$, 0.1 mM dithiothreitol (DTT)) for 60 min at 37 °C. After the incubation, the reaction was stopped by applying 1 μl of 100 mM EDTA and decreasing the temperature to 4 °C. pDNA was decondensed from polycations by applying 1 μl of 10 μg/μl pAsp. Then 2 μl of loading buffer (50% sucrose in distilled water) were applied, and pDNA was then analyzed by gel electrophoresis through 1% (w/v) agarose, followed by staining with ethidium bromide.

Results

Sizes of polycation/pDNA complexes

The particle sizes of pDNA condensed with mu, NLS-mu and PLL at various charge ratios were determined

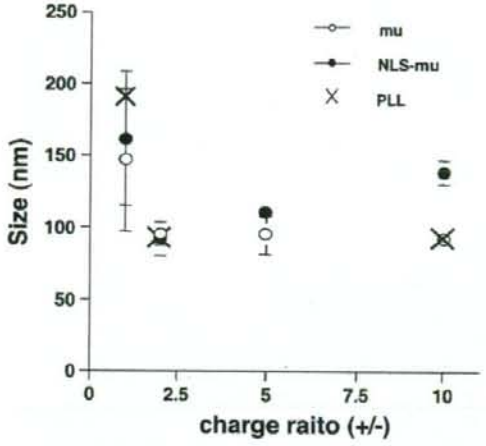

Figure 1. Diameters of the pDNA/polycation complexes. After the preparation of a pDNA complex with NLS-mu, mu and PLL at various charge ratios, the sizes were determined by quasi-elastic light scattering by means of an electrophoresis light-scattering spectrophotometer. Open circles, closed circles and crosses represent the results for mu, NLS-mu and PLL, respectively. Vertical bars indicate the standard deviation of triplicate experiments

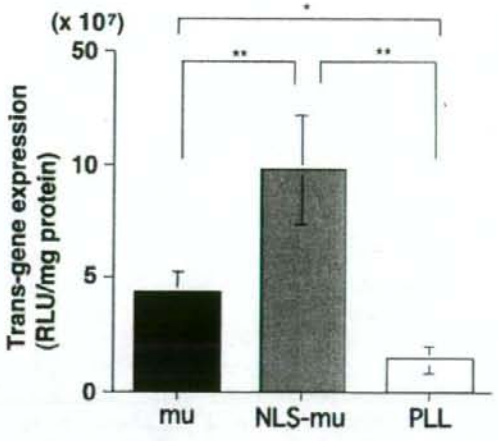

Figure 2. Trans-gene expression by the MEND with various DNA-condensing polycations. pDNA encoding the luciferase reporter gene was condensed with NLS-mu, mu and PLL and further encapsulated into a DOPE/CHEMS lipid layer. These particles were incubated with HeLa cells in serum-free medium and trans-gene expression was evaluated, as described in Materials and Methods. The vertical axis represents luciferase activities expressed as relative light units (RLU) per mg of protein. Closed bars, dotted and open bars represent the results for mu, NLS-mu and PLL, respectively. Vertical bars indicate the standard deviation for triplicate experiments. * and ** represent the significant differences determined by analysis of variance (ANOVA) followed by Student's t-test (*$P < 0.05$; **$P < 0.01$)

by dynamic laser scattering (Figure 1). At a charge ratio of 1, the particle sizes were approximately 150 nm. At a charge ratio of 2, these sizes decreased to ~80 nm. When the charge ratio was further increased, the sizes of the mu particles and PLL particles remained constant or decreased slightly, whereas the size of the NLS-mu particles increased gradually. The mechanism underlying this increase remains to be clarified.

Effect of condensing polycations on transfection activities of the MEND

The effect of DNA condenser on trans-gene expression was compared among NLS-mu, mu and PLL. Transfection activity is rate-limited by various intracellular processes that include cellular uptake, endosomal escape, nuclear transfer and intranuclear transcription [2]. When a simple polyplex is used in a transfection study, it is possible that the difference in the efficiencies of cellular uptake and endosomal escape may affect the transfection activity, and, as a result, the efficiency of nuclear delivery of pDNA cannot be accurately reflected. To minimize these contributions, we applied a recently developed, non-viral multifunctional envelope-type nano device (MEND) [2,11], in which a condensed DNA/polycation complex was coated with a pH-sensitive fusogenic lipid bilayer for the efficient endosomal release of the DNA/polycation core. Since all the particle sizes were minimized to ~80 nm at a charge ratio of 2, the MEND was prepared at this charge ratio. pDNA encoding a luciferase was condensed with these polycations and then coated with a pH-sensitive fusogenic lipid film consisting of DOPE and CHEMS to enhance the endosomal release of the pDNA/polycation complex, as demonstrated previously [11]. The luciferase activities were compared 48 h after the transfection. As shown in Figure 2, luciferase gene expression was increased in the rank order of NLS-mu > mu > PLL. It is particularly noteworthy that the trans-gene expression of the MEND prepared with NLS-mu was approximately 10 times higher than that prepared with PLL.

Cytoplasmic and nuclear microinjection of pDNA condensed with mu, NLS-mu and PLL

To clarify the mechanism for the enhanced trans-gene expression in the MEND prepared with NLS-mu, core particles consisting of the GFP-encoding pDNA and various polycations were microinjected into the cytoplasm. After the condensation of pDNA with NLS-mu, mu and PLL at various charge ratios, pDNA was diluted to 3.3 fmol/μl with injection solution (0.5% RhoDex in H_2O), and then injected into the cytoplasm. At 24 h post-injection, GFP expression was monitored by fluorescence microscopy, and the efficiency of transgene expression in terms of percent of GFP-positive cells to RhoDex-positive cells (E(cyt)) was determined (Figure 3). The most prominent differences in E(cyt) among NLS-mu, mu and PLL were observed at a charge ratio of 2, where the E(cyt) for the mu particles (20.1%) was approximately 1.6 times higher than that of PLL particles (12.3%). A

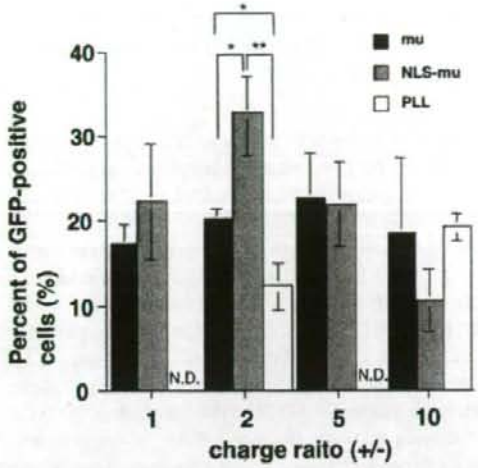

Figure 3. GFP expression after the cytoplasmic microinjection of pDNA condensed with NLS-mu, mu and PLL. After the condensation of the pDNA with NLS-mu, mu and PLL at various charge ratios, 3.3 fmol/μl of the pDNA, mixed with 0.5% RhoDex, were injected to the cytoplasm in HeLa cells. At 24 h post-injection, the ratios of GFP-positive cells to RhoDex-positive cells (E(cyt)) were calculated. Closed bars, dotted bars and open bars represent the results for mu, NLS-mu and PLL, respectively. Typically, 200 cells were injected per experiment. Vertical bars indicate the standard deviation of triplicate experiments. N.D.: not determined. * and ** represent the significant differences determined by ANOVA followed by Student's t-test (*$P < 0.05$; **$P < 0.01$)

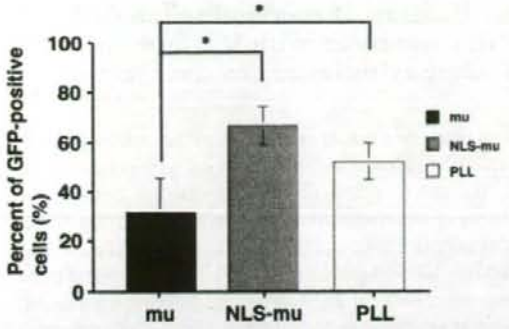

Figure 4. GFP expression after the nuclear microinjection of pDNA condensed with NLS-mu, mu and PLL. After the condensation with pDNA condensed with NLS-mu, mu and PLL, 33 amol/μl of the pDNA, mixed with 0.5% RhoDex, were injected into the nucleus of HeLa cells. At 24 h post-injection, the ratio of GFP-positive cells to RhoDex-positive cells were calculated. In this experiment, RhoDex-positive cells (E(nuc)) were counted just after nuclear microinjection. Closed bars, dotted bars and open bars represent the results for mu, NLS-mu and PLL, respectively. Vertical bars indicate the standard deviation of triplicate experiments. * and ** represent the significant differences determined by ANOVA followed by Student's t-test (*$P < 0.05$)

further increase (2.6 times) was observed for the NLS-mu particles (32.6%). When the charge ratio was increased, the E(cyt) for NLS-mu particles gradually decreased, whereas those for the mu and PLL particles remained constant.

The nuclear transcription efficiencies of pDNA condensed with NLS-mu, mu and PLL at a charge ratio of 2 were subsequently evaluated by nuclear microinjection at 33 amol pDNA/μl with 0.5% RhoDex. To avoid cases where the number of nuclear-injected cells is underestimated by the diffusion of RhoDex from nucleus to the cytosol after 24 h post-injection, the number of cells in which RhoDex was injected into the nucleus was counted immediately after the injection. The efficiency of transgene expression in terms of percent of GFP-positive cells (E(nuc)) was calculated by dividing the number of GFP-positive cells by the number of nuclear RhoDex-positive cells. As shown in Figure 4, the E(nuc) in the NLS-mu particles was not significantly different from that for PLL (73.6 and 57.7%, respectively), whereas that for mu particles was decreased to 35.0%.

Evaluation of nuclear transfer efficiency in terms of nuclear transfer score (NT score)

Considering that pDNA can only be transcribed in the nucleus, the value of E(cyt) should depend not only on the efficiency of nuclear transfer, but also on intra-nuclear transcription. In contrast, E(nuc) exclusively represents the efficiency of nuclear transcription. Therefore, the NT score, denoted as E(cyt) divided by E(nuc), reflects the efficiency of nuclear transfer. The experimentally observed E(cyt) and E(nuc), and calculated NT scores, are summarized in Table 2. The NT score for NLS-mu particles at a charge ratio of 2 was 2.1 times higher than that of PLL, suggesting that NLS-mu particles are more efficiently delivered to the nucleus than PLL. Unexpectedly, the NT scores for NLS-mu and mu particles were comparable at a charge ratio of 2. This suggests that the mu domain, but not the NLS_{SV40} domain, participates in the nuclear delivery of pDNA. When the charge ratio of NLS-mu was increased to 10, both E(cyt) and E(nuc) after cytoplasmic and nuclear microinjection decreased (Table 2). Moreover, the NT score at this charge ratio also decreased to approximately 50% (Table 2), suggesting that the excess condensation of pDNA by NLS-mu lowers not only the nuclear transcription process, but the nuclear transfer process, as well.

Table 2. Summary of GFP expression ratios (%) and NT scores

Particle	E(cyt) (%)	E(nuc) (%)	NT score
mu (charge ratio = 2)	20.1	35.0	0.57 (2.71)
NLS-mu (charge ratio = 2)	32.6	73.6	0.44 (2.10)
NLS-mu (charge ratio = 10)	10.5	47.3	0.22 (1.05)
PLL (charge ratio = 2)	12.3	57.7	0.21 (1.00)

NT scores were calculated as the percent of GFP expression after cytoplasmic microinjection (E(cyt)) divided by that after nuclear microinjection (E(nuc)). Relative NT scores to that of PLL are shown in parentheses.

Visualization of rhodamine-labeled pDNA condensed with NLS-mu, mu and PLL after cytoplasmic microinjection

To visualize the nuclear transfer of pDNA after cytoplasmic microinjection, rhodamine-labeled pDNA condensed with NLS-mu, mu and PLL was injected into the cytoplasm, and the cells were then observed by confocal laser scanning microscopy (CLSM). As a control, naked rhodamine-labeled pDNA was also injected into the cytoplasm. As shown in Figures 5a–5c, rhodamine-labeled pDNA was observed in both the cytoplasm and nucleus as dot-shaped forms, when injected in condensed forms. In the case of naked DNA, the pDNA diffused away from the injected site and was barely detectable in the nucleus as dot-shaped forms under the same image-capture conditions of CLSM (Figure 5d). These data suggest that pDNA, when condensed with polycations, is able to translocate through the nuclear membrane in a condensed form.

Comparison of protection effect of polycations from enzymatic digestion of pDNA by DNase I

It is possible that the NT score and transfection activity can be affected by the extent of enzymatic degradation of pDNA by cytoplasmic nucleases [7,12]. Therefore, the resistance of condensed pDNA to enzymatic digestion by DNase I was evaluated by agarose gel electrophoresis (Figure 6). In DNase I-free conditions, comparable amounts of the free form of pDNA migrated compared with that of naked DNA, when pDNA/polycations particles were decondensed with pAsp (lanes 2, 5, 9 and 13). This suggests that treatment with 1 μg/μl of pAsp can completely decondense pDNA. When naked pDNA was incubated with 0.05 U of DNase I for 60 min, it was completely degraded (lane 2 vs. lane 3). In contrast, when the pDNA/polycation complex was incubated with DNase I, intact pDNA was predominantly observed even after the

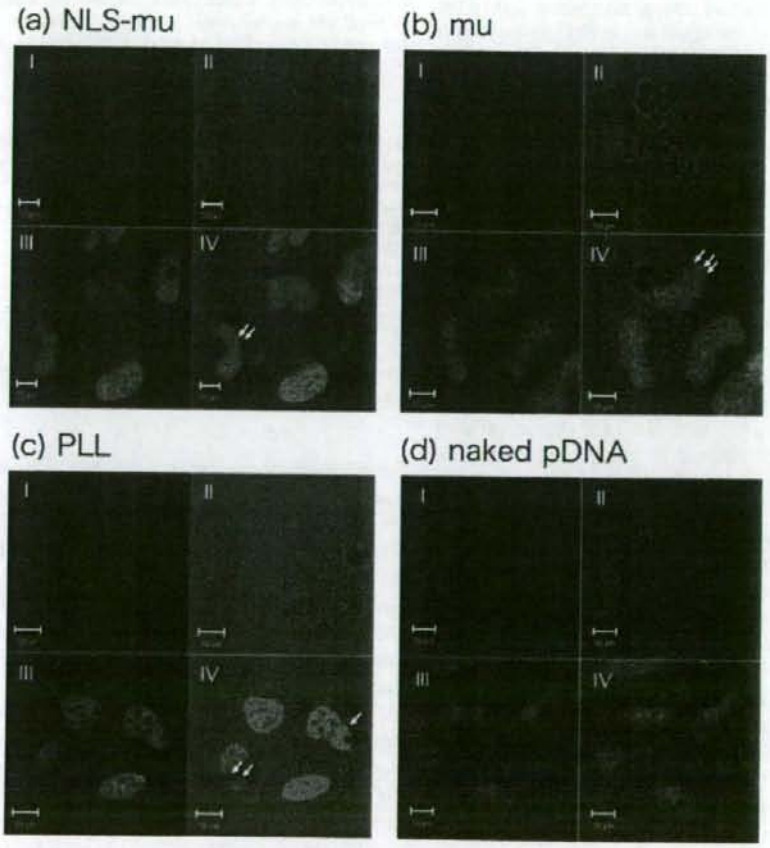

Figure 5. Intracellular distribution of rhodamine-labeled pDNA after cytoplasmic microinjection. Rhodamine-labeled pDNA (26.4 fmol/μl) condensed with NLS-mu (a), mu (b) and PLL (c) at a charge ratio of 2 was injected into the cytoplasm. As a control, naked rhodamine-labeled pDNA was also injected (d). At 1 h post-injection, cells were incubated with 0.5 μM SYTO24 for 15 min to stain the nucleus. Rhodamine-labeled pDNA condensed with NLS-mu (a), mu (b) and PLL (c) was detected in both the cytoplasm and the nucleus (indicated by arrow) as dot-shaped forms 1 h after cytoplasmic microinjection. In contrast, after the microinjection of naked DNA, fluorescence was barely detectable as dot-shaped forms in the nucleus (d). I, II, III and IV represent rhodamine-labeled pDNA, phase-contrast, SYTO24-labeled nucleus and combined image, respectively

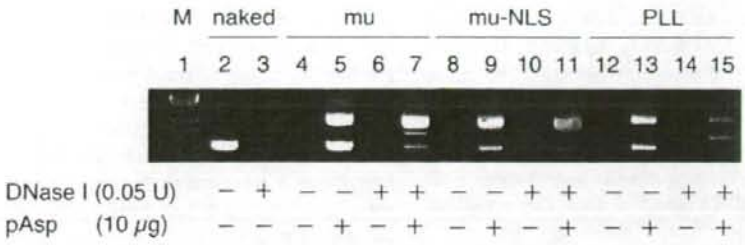

Figure 6. Resistance of pDNA condensed by polycations to enzymatic degradation by DNase I. Naked pDNA (0.4 μg) (lanes 2 and 3) and pDNA condensed with various polycations (lanes 4–7, mu; lanes 8–11, NLS-mu; lanes 12–15, PLL), at a charge ratio of 2, was incubated with (lanes 3, 6–7, 10–11 and 14–15) or without (lanes 1, 4–5, 8–9 and 12–13) 0.05 U of DNase I at 37 °C for 60 min. Digestion was stopped by the addition of 10 mM EDTA and incubation at 4 °C. pDNA was further incubated for 5 min with (lanes 5, 7, 9, 11, 13 and 15) or without (lanes 2–4, 6, 8, 10, 12 and 14) 1 μg/μl pAsp. pDNA was analyzed by gel electrophoresis through 1% (w/v) agarose, followed by staining with ethidium bromide

DNase I treatment (lane 5 vs. lane 7, lane 9 vs. lane 11, and lane 13 vs. lane 15), suggesting that the polycations used in the present study are able to protect pDNA from enzymatic digestion by DNase I.

Discussion

During the past 20 years, it has become clear that the nuclear membrane severely limits trans-gene expression by non-viral vectors [1,2]. In contrast to the adenovirus, which can insert its genomic DNA into the nucleus even in non-dividing cells [13–15], the nuclear entry of the pDNA is severely limited except in the M-phase, during which period the nuclear membrane is temporarily perturbed [3–6]. Therefore, for the development of promising gene delivery systems, efficient nuclear delivery systems for plasmid DNA are highly desired.

To enhance nuclear delivery, the condensation of pDNA with nuclear-targeting polycations is one of the most promising strategies. The pre-condensation of pDNA with cationic peptides modified with M9 derived from heterogeneous nuclear ribonucleoprotein-A1 [16], TAT oligomer [17], protamine [18,19] and a tetramer of NLS_{SV40} [20] have all been reported to enhance the trans-gene expression mediated by lipoplex and/or a polycation. As a candidate for the potent nuclear-targeting polycations, we prepared the novel polycation: NLS-mu, based on the hypothesis that the tight and stable condensation of pDNA caused by mu [10] may enable NLS_{SV40} to be displayed on the surface of a particle, thus permitting it to be recognized by importin.

The effect of the condensing polycation on trans-gene expression by a MEND was first compared. In the present study, polycation/pDNA complexes were encapsulated into the pH-sensitive fusogenic lipid layer (DOPE/CHEMS) to permit the cytoplasmic release of the complexes from the endosome/lysosome [21]. In this system, cellular uptake and endosomal release are dependent on the lipid bilayer. As a result, the efficiencies of these processes would be expected to be comparable regardless of the polycation used in the DNA core, and the potential of polycations for the nuclear delivery is reflected by the transfection activity. As shown in Figure 2, the trans-gene expression of the MEND was in the expected rank order of NLS-mu > mu > PLL, suggesting that NLS-mu would be a useful device for the nuclear targeting of pDNA. However, the issue of whether NLS-mu functions as a useful cargo of pDNA to the nucleus remains unclear, since the condensation could also be attributed to unexpected side effects such as an enhancement in the stability of pDNA [12].

To evaluate the utility of polycations as a nucleus-targeting cargo of pDNA, we investigated efficiency of trans-gene expression in terms of the percent of GFP-positive cells after cytoplasmic microinjection (E(cyt)). As shown in Figure 3, the rank order of the E(cyt) values was quite comparable to that by the trans-gene expression by the MEND. This also suggests the utility of NLS-mu as a nuclear-targeting device. Furthermore, these data allow us to confirm that the microinjection of pDNA/polycations was adequately demonstrated from the technical point of view. As shown in Figure 5, these condensed particles were detected as dot-shaped forms in the nucleus (Figures 4a–4c), whereas naked DNA was barely detectable (Figure 4d), suggesting that pDNA/polycation condensed particles are delivered to the nucleus in a condensed form.

However, E(cyt) values are also a hybrid parameter of the efficiency of cytoplasmic degradation, nuclear transfer and the subsequent intra-nuclear transcription. When pDNA was condensed by means of polycations, it was largely intact even after treatment with DNase I, regardless of the type of polycation used (Figure 6). Thus, E(cyt) is likely to be affected by the latter two processes. To evaluate nuclear transfer and nuclear transcription, separately, we introduced the NT score, denoted as E(cyt) (represented in Figure 3) divided by E(nuc) (represented in Figure 4), as demonstrated previously [22,23]. It should be noted that the NT score does not refer to what fraction of cytoplasm-injected pDNA can be transferred to the nucleus, since this value is dependent on the dosage used for cytoplasmic and nuclear microinjection. However, when NT scores were determined using a fixed dose, these scores could be used as an index of the relative potential as a nuclear transfer device. As a result, pDNA